

## Chapter 4

### *Determination of nAChR stoichiometry using Normalized Försters Resonance Energy Transfer (NFRET)*

Försters resonance energy transfer (FRET) has become a technique widely used in the biological community to assay for protein-protein interactions. FRET describes the distance dependent, non radiative transfer of energy between a donor fluorophore in an excited state and an acceptor fluorophore in the ground state [40]. Donor fluorophores emit at wavelengths that overlap with the acceptor excitation spectrum. In biological applications these donor and acceptor molecules are frequently fluorescent protein variants of GFP. The Förster distance,  $R_0$ , is the distance at which energy transfer is 50% of the maximum, and for fluorescent proteins this distance tends to fall within a range of 40 – 60 Å. Within this distance, detection of a FRET signal is sufficient to indicate interaction between two independent FP labeled proteins [41-42].

FRET is sometimes called a “molecular ruler” as it can be used to directly measure the distances between donor and acceptor fluorophores [43]. This is especially useful when measuring conformational changes before and after ligand binding or during denaturation [44-45]. The distance between FRET donor and acceptor molecules can be simply calculated by equation 1. Where  $E_{FRET}$  is the efficiency of energy transfer,  $\tau_D$  is the decay rate of the donor in the absence of acceptor,  $R_0$ , is the distance at which energy transfer is 50% efficient, and  $r$  is the distance between donor and acceptor fluorophores.

$$(eq\ 1) \quad E_{FRET} = \frac{1}{\tau_D} \left( \frac{R_0}{r} \right)^6$$

This is a simplification from the greater equation given below for rate of FRET,  $k_T(r)$ , between a single donor, D, and acceptor, A, separated by a distance,  $r$ , where  $Q_D$  is the quantum yield of the donor,  $\kappa^2$  is the orientation factor for the donor and acceptor transition dipoles, and  $N$  is Avogadro's number.  $F_D(\lambda)$  is the corrected fluorescence intensity of the donor in the wavelength range  $\lambda$  to  $\lambda+\Delta\lambda$ , and  $\epsilon_A(\lambda)$  is the extinction coefficient of the acceptor at  $\lambda$ .  $n$  represents the refractive index of the medium and is assumed to be 1.4 for biological applications.

$$(eq\ 2) \quad k_T(r) = \frac{Q_D \kappa^2}{\tau_D r^6} \left( \frac{9000(\ln 10)}{128\pi^5 N n^4} \right) \int_0^\infty F_D(\lambda) \epsilon_A(\lambda) \lambda^4 d\lambda$$

Qualitatively, FRET can be used to determine whether two proteins come close enough together to form an interaction. If two FP labeled proteins are in close proximity, such that a FRET signal is detected, it can be implied that they are close enough to form direct interactions with each other. This approach has been applied to nAChRs. Drenan et al. demonstrated that  $\beta 3$  was incorporated into  $\alpha 6^*$  receptors by measuring FRET interactions between FP labeled  $\alpha 6$  and  $\beta 3$  subunits via donor recovery after photobleaching (DRAP) [22].

Within the nAChR pentamer, there are two possible distances between subunits. For instance, in the  $\alpha 6\alpha 4\beta 2\beta 3$  receptor  $\alpha 6$  subunits can be either adjacent, or non-adjacent to  $\beta 3$  subunits. When a receptor contains a single donor and acceptor FP pair there are two possible FRET outcomes that correspond to distance and position within the pentamer. Son et al. estimates that the distance ( $r$ ) between adjacent subunits,  $a$ , is approximately 5.2 nm and  $b$ , the diagonal distance between nonadjacent subunits is approximately 8.3 nm. Using

mEGFP and mCherry, and the donor and acceptor fluorophores,  $R_0 = 5.1$  nm, and equation 3 (a rearrangement of eq. 1)  $E_{FRET}$  is calculated to be 47% for adjacent FP and 5% for non-adjacent FP-labeled subunits. Therefore, it is theoretically possible to determine the position of an  $\alpha 6$ -mEGFP with respect to a  $\beta 3$ -mCherry subunit within an assembled pentamer.

$$(eq. 3) \quad E_{FRET} = \frac{\left(\frac{R_0}{r}\right)^6}{1 + \left(\frac{R_0}{r}\right)^6}$$

The  $\alpha 4\beta 2$  receptor presents additional challenges to interpretation of FRET data because it can be expressed in multiple stoichiometries of two or more of a single subunit subtype. When  $\alpha 4\beta 2$  receptors are expressed with FP labeled  $\alpha 4$  subunits, the  $\alpha 4$  may contain either a mEGFP or mCherry label. Possible label geometries are illustrated in figure 4.1. Nevertheless, from measurements of  $\alpha 4$  subunits labeled with the FRET donor/acceptor pair cyan fluorescent protein (CYP)/ yellow fluorescent protein (YFP), Son et al. proposed that the  $(\alpha 4)_2(\beta 2)_3$  and  $(\alpha 4)_3(\beta 2)_2$  stoichiometries can be differentiated using FRET [6].

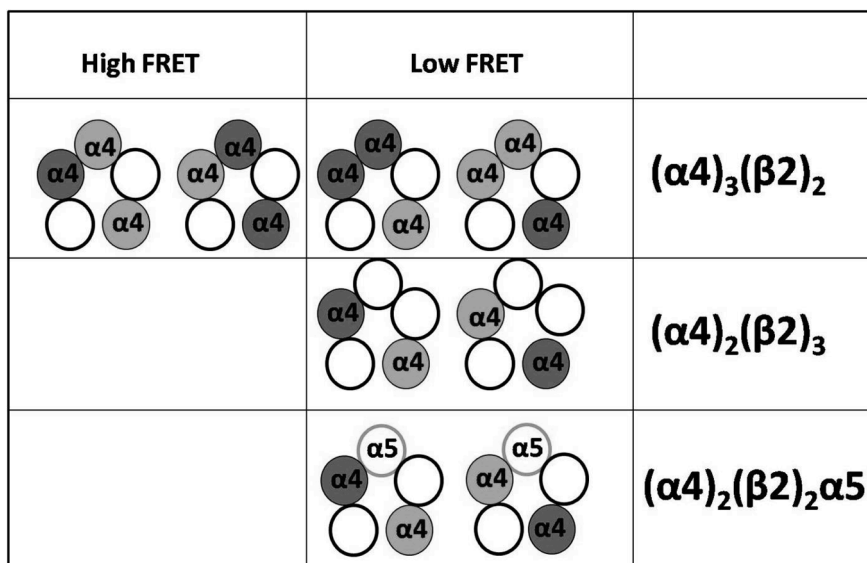


**Figure 4.1**  
Cartoon of  $\alpha 4\beta 2$  and  $\alpha 5\alpha 4\beta 2$  receptor pentamers, their stoichiometries and relative FRET values. Dark grey indicates a FRET donor, light grey indicates a FRET acceptor.

The calculation of  $E_{\text{FRET}}$  in the presence of multiple donor and acceptor molecules is complicated. In their analysis Son et al. make some necessary geometric assumptions:

1. "In a functional  $\alpha 4\beta 2$  receptor, there are at least two agonist binding sites at the  $\alpha$ - $\beta$  subunit interfaces (these are polarized, requiring particular faces of each subunit; see assumption 2 below). Therefore, in the  $(\alpha 4)_2(\beta 2)_3$  stoichiometry, the two  $\alpha 4$  subunits are nonadjacent, and in the  $(\alpha 4)_3(\beta 2)_2$  stoichiometry, the two  $\beta 2$  subunits are nonadjacent.
2. The  $\beta$  subunit is adjacent, in the clockwise direction, to the  $\alpha$  subunit.
3. Although the intracellular domain of the  $\alpha 4$  subunit has roughly twice as many amino acids as that of the  $\beta 2$  subunit, the fluorophores are positioned in an equilateral pentagonal structure.
4. All  $\alpha 4$  subunits are radially equivalent, and all  $\beta 2$  subunits are radially equivalent.
5. Because YFP (acceptor) and CFP (donor) differ by only nine amino acids, YFP- and CFP-tagged subunits are synthesized with equal efficiency and assemble

*randomly within receptor pentamers. The expected results are rather insensitive to departures from this assumption by even 2-fold.*

6. *Again, because YFP and CFP differ only subtly, the structure of an  $\alpha$ 4CFP subunit is the same as  $\alpha$ 4YFP; in addition, a  $\beta$ 2CFP subunit has the same structure as a  $\beta$ 2YFP subunit.*
7. *In a rigorous analysis, the dipole orientation factor  $\kappa^2$  differs between adjacent and nonadjacent subunit pairs. Analysis shows that, in general, the ratio  $\kappa^2$  (nonadjacent subunits)/ $\kappa^2$  (adjacent subunits) lies between 1 and 2; a full prediction requires knowledge of the dipole orientation, which we do not know. We assume that this ratio always equals 1.” [6]*

Using these assumptions, the difference in calculated  $E_{\text{FRET}}$  was dependent on the number of donor and acceptor subunits within the pentamer. Son et al. chose to examine the case in which only the  $\alpha$ 4 subunits are labeled with FPs. An assembled pentamer of  $(\alpha 4)_2(\beta 2)_3$  stoichiometry, contains only one possible arrangement of donor and acceptor FPs. The theoretical  $E_{\text{FRET}}$  calculated from equation 3 for a single mEGFP/mCherry pair in a non-adjacent arrangement is 5%.

The  $(\alpha 4)_3(\beta 2)_2$  stoichiometry, however, can assemble into four possible geometries (see figure 4.1). The measured  $E_{\text{FRET}}$  for a population of  $\alpha 4$ -mEGFP  $\alpha 4$ -mCherry $\beta 2$  receptors in an  $(\alpha 4)_3(\beta 2)_2$  stoichiometry becomes the weighted sum of the  $E_{\text{FRET}}$  for each geometry times the probability of the occurrence of the geometry. The theoretical  $E_{\text{FRET}}$  for each receptor conformation can be calculated using the equations below:

$$(eq. 4) \quad E_{\text{FRET}} (1 \text{ donor, nonadjacent to } 2 \text{ acceptors}) = \left( \frac{2 \left( \frac{R_0}{b} \right)^6}{1 + 2 \left( \frac{R_0}{b} \right)^6} \right)$$

$$\text{(eq. 5) } E_{\text{FRET}} \text{ (1 donor, adjacent and nonadjacent to 2 acceptors)} = \left( \frac{R_0^6 \left( \frac{1}{a^6} + \frac{1}{b^6} \right)}{1 + R_0^6 \left( \frac{1}{a^6} + \frac{1}{b^6} \right)} \right)$$

$$\text{(eq. 6) } E_{\text{FRET}} \text{ (2 donors, both nonadjacent to an acceptor)} = \left( \frac{\left( \frac{R_0}{b} \right)^6}{1 + \left( \frac{R_0}{b} \right)^6} \right)$$

$$\text{(eq. 7) } E_{\text{FRET}} \text{ (2 donors, each adjacent and nonadjacent to 1 acceptor)} = \frac{1}{2} \left( \frac{\left( \frac{R_0}{a} \right)^6}{1 + \left( \frac{R_0}{a} \right)^6} + \frac{\left( \frac{R_0}{b} \right)^6}{1 + \left( \frac{R_0}{b} \right)^6} \right)$$

Normalized Förster Resonance Energy Transfer (NFRET) has been used successfully to examine changes in between  $\alpha 4$  subunits ( $\alpha 4$ -EGFP and  $\alpha 4$ -mCherry) in cells transiently transfected with  $\alpha 4$  and  $\beta 2$  subunits and has provided clues to stoichiometric changes upon addition of pharmacological agents such as nicotine [46]. Detection of FRET is possible by measuring intensity of sensitized emission. Equation 8 describes the calculation of  $E_{\text{FRET}}$  based on intensity measurements.  $I_{\text{FRET}}$  is the intensity of the FRET signal,  $I_{\text{D}}$  is the measured fluorescent intensity of the donor fluorophore,  $BT_{\text{D}}$  is the bleed-through fluorescence detected in the acceptor channel after excitation of the donor.  $I_{\text{A}}$  is the fluorescent intensity of the acceptor fluorophore and  $BT_{\text{A}}$  is the bleed-through fluorescence of the acceptor.

$$\text{(eq. 8) } E_{\text{FRET}} = I_{\text{FRET}} - I_{\text{D}}BT_{\text{D}} - I_{\text{A}}BT_{\text{A}}$$

NFRET describes the measured  $E_{\text{FRET}}$  value after normalization with the square root of  $I_D$  and  $I_A$  (equation 9). This method is ideal for calculation of FRET within a multi-pixel image in which each image pixel may contain different numbers of FP labeled receptors and therefore display different fluorescence intensities [47].

$$(eq. 9) \quad E_{\text{NFRET}} = \frac{I_{\text{FRET}} - I_D B T_D - I_A B T_A}{\sqrt{I_D I_A}}$$

To examine the efficiency of unlabeled  $\alpha 5$  subunits into  $\alpha 4$ -mCherry $\alpha 4$ -mEGFP $\beta 2$  receptors, N2a cells were transiently transfected with DNA constructs of  $\alpha 4$ -mCherry,  $\alpha 4$ -mEGFP, and  $\beta 2$  subunits. Plasmid DNA constructs were transfected in a 1:1:1 ratio of  $\alpha 4$ -mCherry: $\alpha 4$ -mEGFP: $\beta 2$  to bias assembly of the  $(\alpha 4)_3(\beta 2)_2$  stoichiometry. 48 h post-transfection, cells were imaged at 37 °C on an Eclipse C1si laser-scanning confocal microscope with a 63 X, 1.4 numerical aperture, violet-corrected plan apochromatic oil objective and a multianode photomultiplier tube with 32 channels (Nikon Instruments Inc., Melville, NY). Images were linearly unmixed with the emission spectra of the donor and acceptor fluorophores using reference spectra. NFRET was measured using the PixFRET plugin for ImageJ [40, 47]. The calculated NFRET values per-cell were then plotted as average histograms and fitted to two Gaussian curves (see figure 4.2).

It was hypothesized that incorporation of unlabeled, wild-type  $\alpha 5$  constructs into  $\alpha 4$ -mCherry $\alpha 4$ -mEGFP $\beta 2$  parent receptors could be detected as a shift in calculated FRET values. Addition of an unlabeled  $\alpha 5$  subunit into an  $\alpha 4$ -mCherry $\alpha 4$ -mEGFP $\beta 2$  receptor population would lock the FP-labeled  $\alpha 4$  subunits geometries into a non adjacent position

and thus reduce the measured  $E_{\text{NFRET}}$  for the receptor population. N2a cells were transiently transfected with DNA constructs of  $\alpha 4$ -mCherry,  $\alpha 4$ -mEGFP,  $\beta 2$ wt and either  $\alpha 5$  or  $\beta 3$  subunits and compared to the  $\alpha 4$ -mCherry $\alpha 4$ -mEGFP $\beta 2$  control. However, no change in NFRET values or in the areas of the two Gaussians fit to the NFRET histogram was seen (figure 4.2).

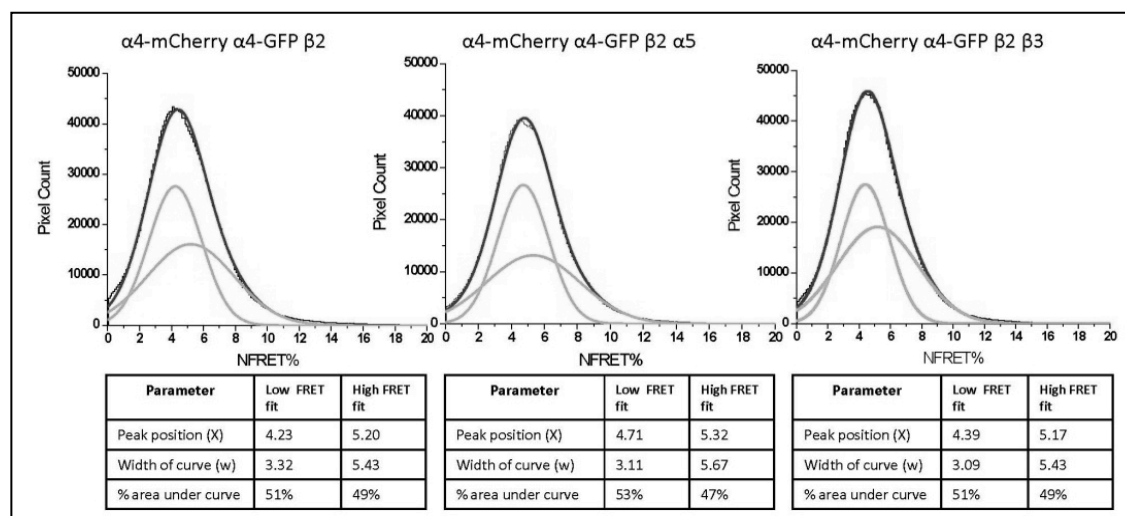


**Figure 4.2**

Sum histograms of NFRET calculated from images of N2a cells expressing fluorescent nAChRs. Each dark grey curve describes the sum NFRET calculated in 40 cells. Light grey curves describe Gaussian curves fit to the sum histogram. Properties of the fit Gaussians were intended to describe each sub population stoichiometry.

It was hypothesized that  $\alpha 4$ -mCherry $\alpha 4$ -mEGFP $\beta 2$  receptors may not incorporate accessory subunits as efficiently as other receptor subtypes.  $\alpha 3\beta 4$  are also known to incorporate  $\alpha 5$  and  $\beta 3$  accessory subunits [7]. NFRET was assayed in N2a cells expressing  $\alpha 3$ -mCherry $\alpha 3$ -mEGFP $\beta 4$ ,  $\alpha 3$ -mCherry $\alpha 3$ -mEGFP $\beta 4\alpha 5$ , or  $\alpha 3$ -mCherry $\alpha 3$ -mEGFP $\beta 4\beta 3$  subunits. A small shift was seen in the peak position of the second fit, corresponding to the “high-FRET” Gaussian component, but it was not found to be significant (figure 4.3).

It is possible that the incorporation of unlabeled  $\alpha 5$  subunits into  $\alpha 4\beta 2$  parent receptors is so inefficient that  $\alpha 4$ -mCherry $\alpha 4$ -mEGFP $\beta 2\alpha 5$  receptors do not represent a

large enough sub-set of the entire receptor population to change on measured NFRET values.

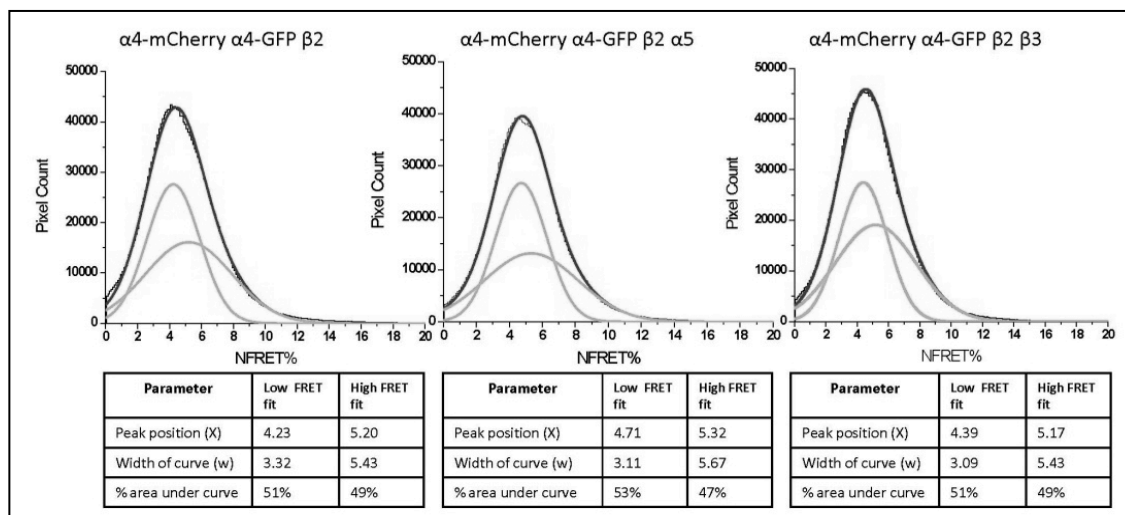


**Figure 4.3**

Sum histograms of NFRET calculated from images of N2a cells expressing fluorescent nAChRs. Each dark grey curve describes the sum NFRET calculated in 40 cells. Light grey curves describe Gaussian curves fit to the sum histogram. Properties of the fit Gaussians were intended to describe of each sub population stoichiometry.

In this case, a direct measurement of the  $\alpha 5^*$  receptor population would be preferable. Detection of interaction between  $\alpha 4$ -mCherry and  $\alpha 5$ -mEGFP could indicate subunit incorporation. NFRET measurements between  $\alpha 5$ -mEGFP378 and  $\alpha 4$ -mCherry were performed in HEK293 cells and yielded inconsistent NFRET signals. NFRET was detected in only 60% of cells imaged, and the peak NFRET value per cell showed high variability using the  $\alpha 5$ -mEGFP378 construct (figure 4.4).

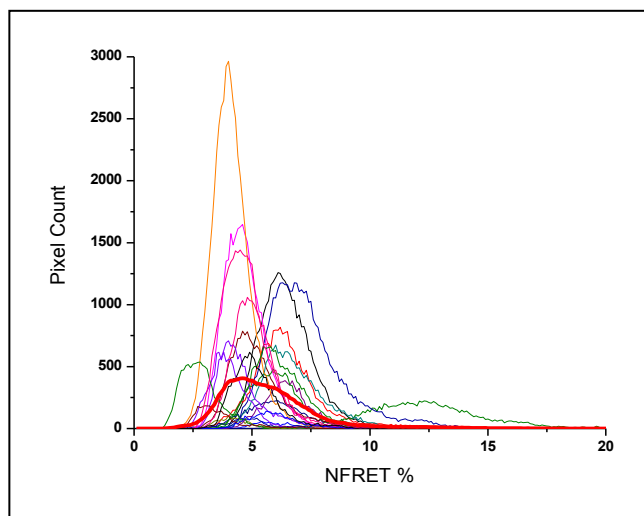


**Figure 4.4**

Same as figure 1.4

23 individual histograms of NFRET positive pixels in images of HEK293 cells expressing  $\alpha 5$ -mEGFP378,  $\alpha 4$ -mCherry, and  $\beta 2$  subunits. Bolded histogram describes the average of all 23 cells.

Distribution of individual cell histograms show significant variability in NFRET calculated for each individual cell. Average peak appears to be near 5% NFRET.

Inconsistency in NFRET data led to the hypothesis that NFRET was not measuring fully-assembled nAChR pentamers but that NFRET measurements were dominated by intracellular sub-assemblies of dimers, trimers, and tetramers. To test this hypothesis, a series of transfections was performed with  $\alpha 4$  or  $\alpha 5$  subunits in the absence of  $\beta 2$ . Without the  $\beta 2$  subunit it is impossible for a fully formed pentamer to assemble. Figure 4.5 shows that NFRET signals are not indistinguishable by eye when N2a cells are transfected with  $\alpha 4$ -mCherry and  $\alpha 4$ -mEGFP, or  $\alpha 4$ -mCherry  $\alpha 4$ -mEGFP and  $\beta 2$  subunits. However, no statistical difference was found after a two-sample independent t-test between the total FRET positive pixels of these two cell populations ( $p = 0.50$ ) (see also appendix iii).

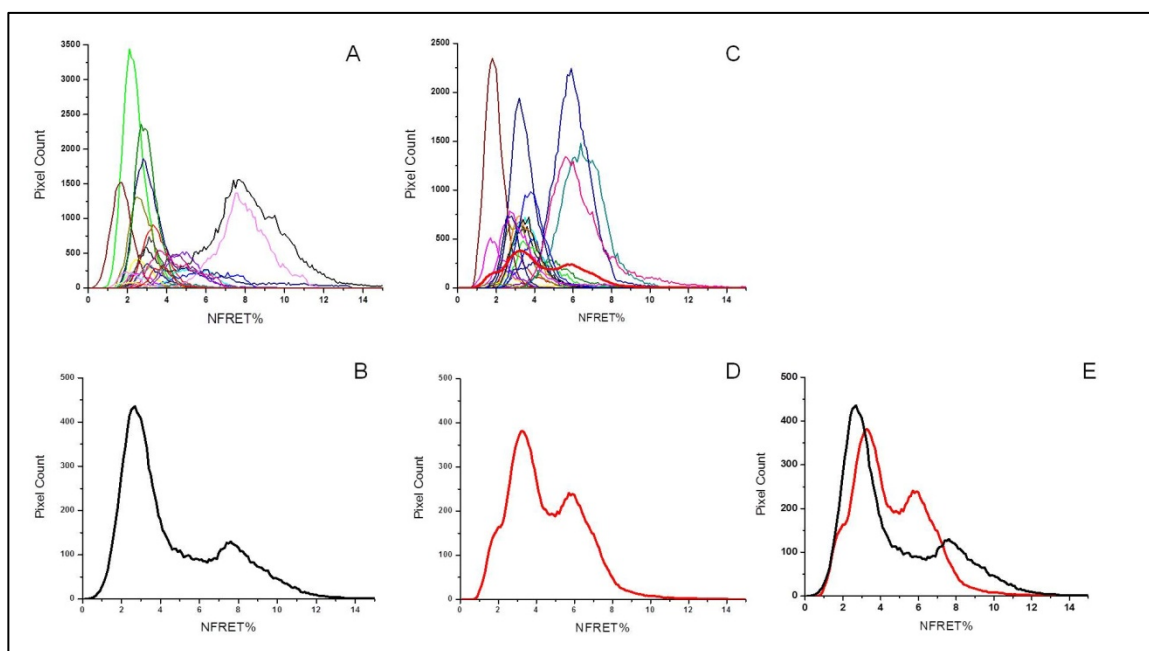


**Figure 4.5**

A. Raw fit histograms of NFRET from  $\geq 40$  N2a cells expressing  $\alpha 4$ -mEGFP and  $\alpha 4$ -mCherry without  $\beta 2$ . Bolded line indicates the average of the raw fits.

B. Average fit histogram of cells described in A.

C. Raw fit histograms of NFRET from  $\geq 40$  N2a cells expressing  $\alpha 4$ -mEGFP and  $\alpha 4$ -mCherry and  $\beta 2$ . Bolded line indicates the average of the raw fits.

D. Average fit histogram of cells described in C.

E. Overlay of average fit histograms for NFRET calculations in cells that do have the ability to form complete  $\alpha 4\beta 2$  pentamers (C and D, light grey line) and cannot form complete pentamers (A and B, dark grey line).

NFRET measurements were performed on N2a cells expressing either  $\alpha 4$ -mCherry and  $\alpha 5$ -mEGFP, or  $\alpha 4$ -mCherry  $\alpha 5$ -mEGFP and  $\beta 2$  subunits with similar results. Figure 4.6 shows an overlay of average NFRET histograms for both the  $\alpha 5$ -mEGFP $\alpha 4$ -mCherry and  $\alpha 5$ -mEGFP $\alpha 4$ -mCherry $\beta 2$  conditions. No statistical difference was found after a two-sample independent t-test between the total FRET-positive pixels in the  $\alpha 5$ -mEGFP $\alpha 4$ -mCherry vs.  $\alpha 5$ -mEGFP $\alpha 4$ -mCherry $\beta 2$  cell populations ( $p = 0.90$ ) or of mean FRET values of  $\alpha 5$ -mEGFP $\alpha 4$ -mCherry expressing cells vs.  $\alpha 5$ -mEGFP $\alpha 4$ -mCherry $\beta 2$  expressing cells ( $p = 0.35$ ) (appendix iii).

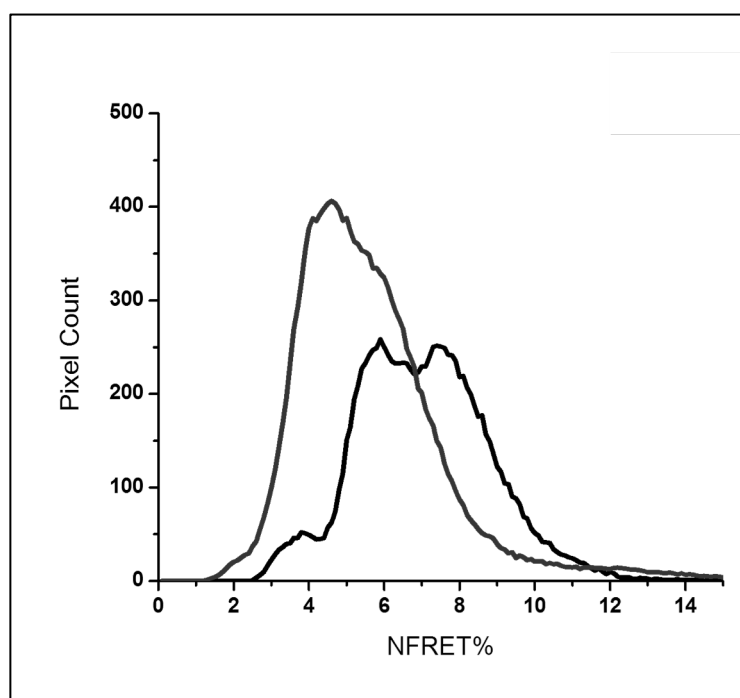


Figure 4.6

Overlay of average fit NFRET histograms from  $\geq 40$  N2a cells expressing  $\alpha 5$ -mEGFP and  $\alpha 4$ -mCherry without  $\beta 2$  (dark grey line), or with  $\beta 2$  (light grey line).

No statistical difference was seen in the two populations leading to the conclusion that NFRET may not be a reflective measure of receptor stoichiometry, but instead may indicate number and composition of intracellular receptor sub-assemblies.

Taken together, these data suggest that the measured NFRET is not reflective of assembled pentameric receptor complexes, but are primarily dimers or other incomplete assemblies. We conclude that NFRET signals are disproportionately influenced by unpaired subunits, possibly in intracellular compartments, and cast doubt on the eligibility of this

technique for use in stoichiometric determination of assembled nAChR receptor complexes as proposed by Son et al., and Srinivasan et al. [6, 23]. Using NFRET we have successfully demonstrated that  $\alpha 5$ -mEGFP and  $\alpha 4$ -mCherry do interact within the cell. This may indicate that  $\alpha 5$ -mEGFP assembles with  $\alpha 4$ -mCherry and  $\beta 2$  to form a complete receptor pentamer, but no assumptions can be made about stoichiometry using this approach.